

APPLICATION OF SEMI-EMPIRICAL MODEL TO ANALYSIS OF VORTEX-EXCITED VIBRATIONS OF BEAMS NEAR SYNCHRONISATION REGION

Roman Lewandowski

Institute of Structural Engineering, Poznan University of Technology, Poznan, Poland

Abstract

This paper presents, the possibility of using a semi-empirical model similar to that proposed by Simiu and Scanlan to analyse the vortex-induced vibrations of beams. In particular, the behaviour of beams near and in the synchronisation region is considered. The motion equations of the system (beam and air) are obtained using the finite element method and the strip method. The aerodynamic excitation forces perpendicular to the wind flow direction are considered as a sum of forces due to the turbulence of oncoming flow, the forces caused by the vortex shedding and forces caused by the air-structure interaction. The forces due to the air-structure interaction are described by means of the model proposed by Simiu and Scanlan. The excitation forces caused by turbulence and by the vortex shedding are described using the Fourier series in time. The Fourier components of time series are determined on the basis of the appropriate power spectral density functions given in the literature. The time integration method is used to obtain the transient and steady state solutions of motion equations. Several exemplary solutions for beams with cylindrical cross-section are obtained in the above-mentioned way. The results of calculations indicate that the typical dynamic behaviour of beams, observed in experiments, can be modelled if the aerodynamic constants appearing in the semi-empirical model have been appropriately chosen.

1. Introduction

A recent trend in civil engineering is to build slender and lighter structures, which are often flexible and weakly damped. The example structures of this class are steel chimneys, bridge pylons and tall buildings. Due to their mechanical properties, these structures are very sensitive to wind. In some cases they can vibrate with large amplitudes which are very dangerous for the structure. One type of dangerous vibrations is known as the lock-in phenomenon. The vibrations of this type are the results of wind passing round a bluff body and forming an aerodynamic wake. As the shedding frequency is approximately equal to one of the natural frequencies of the structure, the structure begins to vibrate with large amplitudes in the plane perpendicular to the undisturbed flow direction. The results of experimental works

with a rigid cylinder exposed to air flow, described for example by Goswami et al. [1], show that the responses of the cylinder are periodic in the synchronisation region and they are modulated or multi-harmonic outside this region.

Winds are unsteady and manifest random fluctuations in both space and time domains. It is well-known that wind fluctuations can be considered as a stationary process in the time domain and a non-homogenous process in the space domain. Consequently, winds are characterised by their statistical properties and the responses of structures to wind actions can be described using the stochastic approach (see, for example, [2]). In the context of vortex-induced vibrations this approach is used by Vickery and Basu [3,4]. Moreover, thanks to modern computer technology it is possible to generate, on the basis of the known wind spectral density function, the exemplary time histories of wind fluctuations and analyse the structure behaviour in the time domain.

The problem of vortex-induced vibrations was analysed by Baroush et al.[5] and Dul et al. [6] who used empirical aerodynamic models and the time integration methods to determine steady state vibrations of beams in the synchronisation region. The periodic steady state vibrations of beams in the lock-in region were also studied by Lewandowski [7] who used both the harmonic balance method and the Newmark method. In this paper only the periodic responses of structures are discussed because the harmonic with shedding frequency dominates in excitation and the non-linear air-structure interaction significantly increases the same harmonic in the structure response. In the above articles the empirical models proposed by Scanlan and co-workers (see [8]) and by Hartlen and Currie (in paper [7]) are used to describe the main characteristics of aerodynamic forces. The random character of wind is not taken into account in these papers and the excitations due to wind are treated as deterministic and harmonic processes in the time domain. As it was mentioned above, the random character of wind is taken into account by Vickery and Basu in two papers [3,4].

2. Problem formulation

The considered system (the beam and the flow field) is divided into finite elements (beam) and strips (flow field). Each strip is parallel to the direction of undisturbed flow and has a width equal to the finite element length. The strips are also perpendicular to the finite elements. The main assumption is that flows in strips are mutually independent, which means that the aerodynamic forces are induced only by the flow in the associated strip. In this paper the transverse vibrations in the direction of undisturbed wind are neglected and only the cross-wind vibrations of beam are considered.

2.1 Equation of motion

The motion equation of beams derived using the finite element method can be written in the following form:

$$\mathbf{M}\ddot{\mathbf{w}}(t) + \mathbf{C}\dot{\mathbf{w}}(t) + \mathbf{K}\mathbf{w}(t) = \mathbf{F}(t), \quad (1)$$

where the symbols \mathbf{M} , \mathbf{C} , \mathbf{K} , $\mathbf{w}(t)$ and $\mathbf{F}(t)$ denote the mass, damping and stiffness matrices and the vectors of nodal parameters and the excitation forces, respectively. The superscript dot implies differentiation with respect to time t .

In this paper, the typical two node beam finite element is used. Each node has two degrees of freedom (i.e. the transverse displacement w and rotation φ) and the Hermite's polynomials are chosen as the shape functions. The across-wind transverse displacements of finite elements $w(z,t)$ can be described by

$$w(z,t) = \mathbf{N}^T(z)\mathbf{w}_e(t), \quad (2)$$

where $\mathbf{w}_e(t) = \text{col}(w_a, \varphi_a, w_b, \varphi_b)$ is the vector of nodal parameters while w_a , w_b and φ_a , φ_b are displacements and rotations at the left end and right end of the finite elements, respectively. $\mathbf{N}(z) = \text{col}(N_1, N_2, N_3, N_4)$ is the vector of shape functions defined as follows:

$$\begin{aligned} N_1 &= (1 - 3\eta^2 + 2\eta^3), & N_2 &= \eta(1 - \eta)^2, \\ N_3 &= 3\eta^2 - 2\eta^3, & N_4 &= \eta^2(\eta - 1), \\ \eta &= z/l, \end{aligned} \quad (3)$$

and l is the finite element length.

Moreover, it is assumed that the damping matrix is proportional and can be expressed in the following well-known form:

$$\mathbf{C} = \alpha\mathbf{M} + \beta\mathbf{K}, \quad (4)$$

where α and β are some parameters.

2.2 Description of excitation forces

The semi-empirical model proposed by Scanlan and co-workers [1,8] is used to describe the aerodynamic forces. According to this model the across-wind force per unit span acting on the cylinder is

$$\begin{aligned} F(z,t) &= F_1(z,t) + F_2(z,t) + F_3(z,t) \\ &= \frac{1}{2}\rho U^2(z)D(z) \left\{ Y_1(z) \frac{\dot{w}(z,t)}{U(z)} + Y_2(z) \frac{w^2(z,t)\dot{w}(z,t)}{D^2(z)U(z)} \right\} \\ &\quad + \frac{1}{2}\rho U^2(z)D(z)C_L(z,t) + \\ &\quad \frac{1}{2}\rho U^2(z)D(z)C_D(z) \frac{v(z,t)}{U(z)} \end{aligned} \quad (5)$$

where ρ is the air density, $U(z)$ is the mean wind velocity, $D(z)$ is the characteristic cross-section diameter, $v(z,t)$ is the along-wind perturbation of mean wind velocity. Moreover, $Y_1(z)$, $Y_2(z)$, $C_L(z,t)$ and $C_D(z)$ denote the aerodynamic parameters and the lift and drag coefficients, respectively. The aerodynamic parameters are functions of the reduced frequency $K = \omega_n D / U$, where ω_n is the chosen natural frequency of beam. Furthermore, the shedding frequency denoted by ω_s is also introduced. The shedding frequency satisfies the Strouhal relation

$$\omega_s D / U = 2\pi S, \quad (6)$$

where $S \approx 0.20$ is the Strouhal number.

The original version of the discussed model, as it is described by Simiu and Scanlan [8], contains also the term proportional to transverse displacement $w(z,t)$. This term is neglected in the present formulation because it is small compared to the term describing the aerodynamic damping and to the term describing the beam restoring forces.

The first term in equation (5) describes the aerodynamic damping forces due to wind and, in this paper, is considered to be the deterministic one. The nature of the second and third terms is stochastic. The second term describes the effects of vortex shedding in the wake of the structure at rest while the third term describes the effects of spectral turbulence in the oncoming flow.

The vector of equivalent nodal forces is derived in a different way for the deterministic part (i.e. $F_1(z,t)$) and the stochastic parts (i.e. $F_2(z,t)$ and $F_3(z,t)$) of the aerodynamic forces. It is assumed that the mean wind velocity $U(z)$ and the characteristic dimension $D(z)$ are constant on the finite element length. This means that also the aerodynamic parameters $Y_1(z)$ and $Y_2(z)$ are constants. The above mentioned quantities are now denoted as U_e , D_e , Y_{1e} and Y_{2e} , respectively.

The virtual work of the first part of aerodynamic forces at time t can be written as

$$\delta L_1 = \int_0^l \frac{1}{2} \rho U_e^2 D_e \left[Y_{1e} \frac{\dot{w}(z,t)}{U_e} + Y_{2e} \frac{w^2(z,t) \dot{w}(z,t)}{D_e^2 U_e} \right] \delta w(z) dz$$

$$= \delta \mathbf{w}_e^T \left[\mathbf{D}_L^e + \mathbf{D}_{NL}^e(\mathbf{w}_e(t), \mathbf{w}_e(t)) \right] \dot{\mathbf{w}}_e(t), \quad (7)$$

where l is the finite element length, $\delta w(z,t) = \mathbf{N}^T(z) \delta \mathbf{w}_e$ is the variation of displacement and

$$\mathbf{D}_L^e = \frac{1}{2} \rho U_e^2 D_e Y_{1e} \int_0^l \mathbf{N}(z) \mathbf{N}^T(z) dz, \quad (8)$$

$$\mathbf{D}_{NL}^e(\mathbf{w}_e(t), \mathbf{w}_e(t)) = \frac{\rho U_e Y_{2e}}{2 D_e} \int_0^l \mathbf{N}(z) \mathbf{w}_e^T(t) \mathbf{N}(z) \mathbf{N}^T(z) \mathbf{w}_e \mathbf{N}^T(z) dz. \quad (9)$$

After integration, the matrix \mathbf{D}_L^e has the following explicit form:

$$\mathbf{D}_L^e = \frac{\rho l U_e^2 D_e Y_{1e}}{840} \begin{bmatrix} 156 & 22l & 54 & -13l \\ 22l & 4l^2 & 13l & -3l^2 \\ 54 & 13l & 156 & -22l \\ -13l & -3l^2 & -22l & 4l^2 \end{bmatrix}, \quad (10)$$

Finally, the vector of nodal aerodynamic forces $\mathbf{F}_{1e}(t)$ equivalent to those described by the first part of $F(z,t)$ is

$$\mathbf{F}_{1e}(t) = \left[\mathbf{D}_L^e + \mathbf{D}_{NL}^e(\mathbf{w}_e(t), \mathbf{w}_e(t)) \right] \dot{\mathbf{w}}_e(t). \quad (11)$$

The probabilistic characteristics of lift factor $C_L(t)$ and the fluctuations of wind velocity $v(t)$ are needed for proper description of the stochastic parts of aerodynamic forces. The spectral density of the lift coefficient S_{CL} is [8]

$$\frac{n S_{CL}(z,n)}{\bar{C}_L^2} = \frac{1}{\sqrt{\pi} B n_s} \exp \left[- \left(\frac{1-n/n_s}{B} \right)^2 \right], \quad (12)$$

where $n = 2\pi / \omega$, $n_s = 2\pi / \omega_s$, ω is the circular frequency and B is the empirical parameter determining the bandwidth of the spectral curve. Moreover, the symbol $\sqrt{\bar{C}_L^2}$ denotes the rms coefficient of the lift factor C_L . The cross-spectral density of the lift factor can be expressed as

$$S_{CL}(z_1, z_2, n) = \sqrt{S_{CL}(z_1, n) S_{CL}(z_2, n)} \cos(2ar) \exp(-ar^2), \quad (13)$$

where

$$r = \frac{2|z_1 - z_2|}{U(z_1) + U(z_2)}, \quad (14)$$

and a is a measure of the decay of function $S_{CL}(z_1, z_2, n)$ with the distance $|z_1 - z_2|$.

The spectral density function $S_v(z,n)$ of the lateral velocity fluctuations $v(t)$ can be approximated by the formula

$$\frac{n S_v(z,n)}{u_*^2} = \frac{15f}{(1+9.5f)^{5/3}}, \quad (15)$$

where $f = nz / U(z)$ is the Monin co-ordinate and u_* is the shear velocity. The cross-spectral density function of the lateral velocity fluctuations is assumed in the following form:

$$S_v(z_1, z_2, n) = \sqrt{S_v(z_1, n) S_v(z_2, n)} \exp(-\frac{1}{3} \hat{f}), \quad (16)$$

where

$$\hat{f} = \frac{2nC_z |z_1 - z_2|}{U(z_1) + U(z_2)}, \quad (17)$$

and $C_z = 10$. The factor $1/3$ appearing in equation (16) is taken from Simiu and Scanlan (see [8], page 69).

The mean wind velocity on the level Z above the ground is given by

$$U(z) = 2.5 u_* \ln(z / z_0), \quad (18)$$

where z_0 is the roughness length. Sometimes the mean velocity is assumed to be constant along the beam. Moreover, \bar{C}_L , B , a and C_D appearing in relations (5) and (12) - (18) are determined using formulas given in [8].

On the basis of spectral power density functions S_{CL} and S_v given above it is possible to generate both the exemplary wind fluctuations histories $v(z,t)$ and the exemplary histories of the lift factor $C_L(z,t)$ treated as stationary stochastic processes in time. This can be done using the simulation techniques based on the method of superposition of harmonic waves with random phases [10] or using one of the time series methods, for example the autoregressive and moving average method [11]. In this article, the method of superposition of harmonic waves, known also as the spectral representation method, is used to simulate the histories of fluctuations of $v(z,t)$ and $C_L(z,t)$ in time. The detailed description of the applied version of the spectral representation method will be given in the next section.

At this stage it is enough to conclude that the exemplary simulated history of the stochastic parts of aerodynamic forces can be approximated in space and on the level of the finite element in the following way

$$P_e(z,t) = F_2(z,t) + F_3(z,t) =$$

$$N_1(z)p_a(t) + N_3(z)p_b(t), \quad (19)$$

where $p_a(t)$ and $p_b(t)$ are the above mentioned aerodynamic forces on the left and right end of the finite element, respectively. Moreover, $N_1(z)$ and $N_3(z)$ are the shape functions defined by equations (3).

The virtual work of these forces at time t can be written as

$$\begin{aligned} \delta L_{23} &= \int_0^l P_e(z,t) \delta w(z) dz = \\ & \delta \mathbf{w}_e^T \int_0^l \mathbf{N}(z) [N_1(z)p_a(t) + N_3(z)p_b(t)] dz = \\ & \delta \mathbf{w}_e^T \mathbf{P}_e(t). \end{aligned} \quad (20)$$

Finally, the vector of nodal excitation forces caused by the random parts of aerodynamic forces can be written in the following explicit form:

$$\mathbf{P}_e(t) = \frac{1}{420} \begin{bmatrix} 156 p_a(t) + 54 p_b(t) \\ 22 l p_a(t) + 13 l p_b(t) \\ 54 p_a(t) + 156 p_b(t) \\ -13 l p_a(t) - 22 l p_b(t) \end{bmatrix}. \quad (21)$$

The global vector of excitation forces $\mathbf{F}(t)$ can be now written in the form:

$$\mathbf{F}(t) = [\mathbf{D}_L + \mathbf{D}_{NL}(\mathbf{w}(t), \mathbf{w}(t))] \dot{\mathbf{w}}(t) + \mathbf{P}(t), \quad (22)$$

where the matrices \mathbf{D}_L and $\mathbf{D}_{NL}(\mathbf{w}(t), \mathbf{w}(t))$ and the vector $\mathbf{P}(t)$ are the global counterparts of matrices \mathbf{D}_L^e and $\mathbf{D}_{NL}^e(\mathbf{w}_e(t), \mathbf{w}_e(t))$ and the vector $\mathbf{P}_e(t)$, previously defined on a level of finite elements.

Taking into account equation (22), we can rewrite the beam motion equation in the following form:

$$\mathbf{M} \ddot{\mathbf{w}}(t) + \mathbf{C}_{NL}(\mathbf{w}(t), \mathbf{w}(t)) \dot{\mathbf{w}}(t) + \mathbf{K} \mathbf{w}(t) = \mathbf{P}(t), \quad (23)$$

where

$$\mathbf{C}_{NL}(\mathbf{w}(t), \mathbf{w}(t)) = \mathbf{C} - \mathbf{D}_L - \mathbf{D}_{NL}(\mathbf{w}(t), \mathbf{w}(t)). \quad (24)$$

3. Simulation of histories of stochastic excitation forces

In this section, the method of simulation of exemplary histories of random function $h(z,t)$ is described. This function can be either $C_L(z,t)$ or $v(z,t)$ depending on which terms of aerodynamic forces are taken into consideration. It is assumed that the power spectral density

function of $h(z,t)$ is known and denoted by $S(\omega)$. Function $h(z,t)$ can be approximated by a set of functions of time $h_i(t) = h(z_i, t)$, ($i = 1, 2, \dots, m$) at the nodal points along the beam i.e. for $z = z_i$. Now, the vector $\mathbf{h}(t)$ can be build from all $h_i(t)$. We assume that on the finite element level function $h(z,t)$ can be described with a proper accuracy by

$$h(z,t) = N_1(z)h_a(t) + N_3(z)h_b(t), \quad (25)$$

where $h_a(t)$ and $h_b(t)$ are these $h_i(t)$ functions which are defined at the left and right end of the finite element, respectively.

Under these assumptions the vector $\mathbf{h}(t)$ can be treated as a set of stationary Gaussian random processes with zero means and the spectral density matrix $\mathbf{S}(\omega)$. The elements $S_{ij}(\omega)$ of $\mathbf{S}(\omega)$ are given by

$$S_{ij}(\omega) = \sqrt{S_i(\omega)S_j(\omega)} \gamma_{ij}(\omega), \quad (26)$$

where $S_i(\omega)$ is the power spectrum of $h_i(t)$ process and $\gamma_{ij}(\omega)$ is the coherence function. For $C_L(z,t)$ and $v(z,t)$ both functions are given in Section 2.

The correlation matrix $\mathbf{R}(\tau)$ of the vector of random processes $\mathbf{h}(t)$, which is one of the main characteristic of random processes, is defined by

$$\mathbf{R}(\tau) = \lim_{T \rightarrow \infty} \frac{1}{2T} \int_{-T}^T \mathbf{h}(t) \mathbf{h}^T(t + \tau) dt. \quad (27)$$

This matrix can be also calculated on the base of the power spectral matrix $\mathbf{S}(\omega)$. In this case, the elements $R_{ij}(\tau)$ of the matrix $\mathbf{R}(\tau)$ are given by

$$R_{ij}(\tau) = \int_{-\infty}^{\infty} S_{ij}(\omega) \exp(i\omega\tau) d\omega. \quad (28)$$

The vector of random processes $\mathbf{h}(t)$ can be expressed in the form (see [12]):

$$\mathbf{h}(t) = \mathbf{Z} \mathbf{q}(t), \quad (29)$$

where \mathbf{Z} is the matrix of eigenvectors of the correlation matrix $\mathbf{R}(\tau)$ determined for $\tau = 0$. It means that all column vectors \mathbf{z}_i of the matrix \mathbf{Z} satisfy the following equation:

$$[\mathbf{R}(0) - \lambda_i \mathbf{I}] \mathbf{z}_i = \mathbf{0}, \quad (30)$$

where λ_i is the eigenvalue associated with \mathbf{z}_i . The eigenvectors \mathbf{z}_i are normalised in such a way that

$$\mathbf{Z}^T \mathbf{R}(0) \mathbf{Z} = \mathbf{I}, \quad (31)$$

where \mathbf{Z} is the matrix of eigenvectors \mathbf{z}_i and \mathbf{L} is the diagonal matrix of eigenvalues λ_i .

On the other hand it can be shown that the vector of uncorrelated random processes $\mathbf{q}(t)$ appearing in equation (29) is now normalised in such a way that the auto-correlation factor of $q_i(t)$ is equal to the eigenvalue λ_i of the matrix $\mathbf{R}(0)$, respectively. Introducing relation (29) into equation (27) and taking into account the fact that processes $q_i(t)$ are uncorrelated, equation (27) becomes

$$\mathbf{R}(0) = \mathbf{Z}^T \mathbf{C} \mathbf{Z}, \quad (32)$$

where

$$\mathbf{C} = \lim_{T \rightarrow \infty} \frac{1}{2T} \int_{-T}^T \mathbf{q}(t) \mathbf{q}^T(t) dt, \quad (33)$$

is a diagonal matrix. Equation (32) can be rewritten in the form

$$\mathbf{Z}^T \mathbf{R}(0) \mathbf{Z} = \mathbf{C}, \quad (34)$$

because the matrix $\mathbf{R}(0)$ is symmetric and positive definite, $\mathbf{Z}^{-1} = \mathbf{Z}^T$ and $\mathbf{Z}^{-T} = \mathbf{Z}$. Now, comparing equations (31) and (34) we conclude that $\mathbf{C} = \mathbf{L}$.

In the spectral representation method each random process is expressed in the form of the following truncated Fourier series

$$q_i(t) = \sum_{j=1}^N \beta_{ij} \cos(\omega_j t + \theta_{ij}) = \sum_{j=1}^N (a_{ij} \cos \omega_j t + b_{ij} \sin \omega_j t), \quad (35)$$

where θ_{ij} are a set of independent phase angles uniformly distributed between 0 and 2π . The relations between β_{ij} , θ_{ij} and a_{ij} , b_{ij} are $\beta_{ij}^2 = a_{ij}^2 + b_{ij}^2$ and $\tan \theta_{ij} = -b_{ij} / a_{ij}$. Moreover, $\omega_j = (j-1)\delta\omega$, $\delta\omega = \omega_{max} / N$ is the frequency interval, ω_{max} and N are the upper limit of frequencies and the number of frequency intervals, respectively. The frequency band must contain all significant natural frequencies of the structure.

Now, the procedure of determination of uncorrelated and appropriately scaled random processes $q_i(t)$ will be briefly described. First, the coefficients $\tilde{\beta}_{ij}$ are calculated from the formula

$$\tilde{\beta}_{ij} = \sqrt{2S_i(\omega_j)\delta\omega}, \quad (36)$$

and the phase coefficients $\tilde{\theta}_{ij}$ are determined using the generator of random numbers. Next we calculate \tilde{a}_{ij} and \tilde{b}_{ij} from

$$\tilde{a}_{ij} = \tilde{\beta}_{ij} \cos \tilde{\theta}_{ij}, \quad \tilde{b}_{ij} = -\tilde{\beta}_{ij} \sin \tilde{\theta}_{ij}. \quad (37)$$

The wave over $\tilde{\beta}_{ij}$, $\tilde{\theta}_{ij}$ and \tilde{a}_{ij} , \tilde{b}_{ij} means that these quantities describe the random processes $\tilde{q}_i(t)$ which are, in general, correlated and not appropriately scaled.

Let us introduce vectors $\tilde{\mathbf{a}}_i = \text{col}(\tilde{a}_{i1}, \tilde{a}_{i2}, \dots, \tilde{a}_{iN})$ and $\tilde{\mathbf{b}}_i = \text{col}(\tilde{b}_{i1}, \tilde{b}_{i2}, \dots, \tilde{b}_{iN})$. The cross-correlation factor for two correlated processes $\tilde{q}_k(t)$ and $\tilde{q}_l(t)$ is defined by

$$\mu_{kl} = \lim_{T \rightarrow \infty} \frac{1}{2T} \int_{-T}^T \tilde{q}_k(t) \tilde{q}_l(t) dt, \quad (38)$$

from which after introducing equation (35) and calculating the resulting integrals we obtain

$$2\mu_{kl} = \sum_{j=1}^N (\tilde{a}_{kj} \tilde{a}_{lj} + \tilde{b}_{kj} \tilde{b}_{lj}) = \tilde{\mathbf{a}}_k^T \tilde{\mathbf{a}}_l + \tilde{\mathbf{b}}_k^T \tilde{\mathbf{b}}_l. \quad (39)$$

The above cross-correlation factors will be equal to zero and random processes $\tilde{q}_k(t)$ and $\tilde{q}_l(t)$ will be uncorrelated if both terms in relation (39) are separately equal to zero i.e., $\tilde{\mathbf{a}}_k^T \tilde{\mathbf{a}}_l = 0$ and $\tilde{\mathbf{b}}_k^T \tilde{\mathbf{b}}_l = 0$. This means that the considered problem can be reduced to orthogonalization of two sets of vectors $\tilde{\mathbf{a}}_i$ and $\tilde{\mathbf{b}}_i$, ($i = 1, 2, \dots, m$), separately. The process of orthogonalization can be done using the Gram - Schmidt procedure. The Fourier coefficients obtained after the orthogonalization procedure will be denoted by \hat{a}_{ij} and \hat{b}_{ij} or by $\hat{\mathbf{a}}_i$ and $\hat{\mathbf{b}}_i$ if the matrix notation is used. The random processes $\hat{q}_i(t)$ obtained in this way are uncorrelated but they are not appropriately scaled.

The auto-correlation factor of the process $\hat{q}_i(t)$ can be written in terms of \hat{a}_{ij} and \hat{b}_{ij} after introducing relation (35) into equation (33) and calculating the resulting integrals to obtain

$$2\mu_{ii} = \sum_{j=1}^N (\hat{a}_{ij}^2 + \hat{b}_{ij}^2) = \hat{\mathbf{a}}_i^T \hat{\mathbf{a}}_i + \hat{\mathbf{b}}_i^T \hat{\mathbf{b}}_i. \quad (40)$$

From the above equation it is easy to conclude that the random process $\hat{q}_i(t)$ can be normalised in such a way that $\mu_{ii} = \lambda_i$ if the coefficients in the Fourier series (35) are given by

$$a_{ij} = \hat{a}_{ij} \sqrt{\lambda_i / \mu_{ii}}, \quad b_{ij} = \hat{b}_{ij} \sqrt{\lambda_i / \mu_{ii}}. \quad (41)$$

Finally, the history of the stochastic part of aerodynamic force $p_k(t)$ acting on level $z = z_k$ is described by

$$p_k(t) =$$

$$\begin{aligned} & \frac{1}{2}\rho U^2(z_k)D(z_k)\sum_{i=1}^m\sum_{j=1}^N Z_{ki}\left(a_{ij}^C \cos\omega_j t + b_{ij}^C \sin\omega_j t\right) + \\ & \frac{1}{2}\rho U(z_k)D(z_k)C_D(z_k) \\ & \sum_{i=1}^m\sum_{j=1}^N Z_{ki}\left(a_{ij}^v \cos\omega_j t + b_{ij}^v \sin\omega_j t\right), \end{aligned} \quad (42)$$

where the symbol Z_{ki} denotes an element of matrix \mathbf{Z} . Moreover, a_{ij}^C , b_{ij}^C and a_{ij}^v , b_{ij}^v are the Fourier coefficients of exemplary histories of $C_L(z_k, t)$ and $v(z_k, t)$, respectively.

4. Solution of motion equation

The in time integration method is used to obtain both the transient and steady state solutions of the motion equation (23). The well known version of the Newmark method called the average acceleration method is chosen. The method is briefly described in this section.

For convenience, equation (23) is first rewritten in the following form:

$$\mathbf{R}(t) = \mathbf{M}\mathbf{a}(t) + \mathbf{C}_{NL}(\mathbf{w}(t))\mathbf{v}(t) + \mathbf{K}\mathbf{w}(t) - \mathbf{P}(t) = \mathbf{0}; \quad (43)$$

where $\mathbf{R}(t)$ is the residual vector which vanishes in an equilibrium state and $\mathbf{v}(t) = \dot{\mathbf{w}}(t)$, $\mathbf{a}(t) = \dot{\mathbf{v}}(t)$.

The following Newmark formulas:

$$\mathbf{w}_{n+1} = \mathbf{w}_n + \tau\mathbf{v}_n + \frac{1}{4}\tau^2(\mathbf{a}_{n+1} + \mathbf{a}_n), \quad (44)$$

$$\mathbf{v}_{n+1} = \mathbf{v}_n + \frac{1}{2}\tau(\mathbf{a}_{n+1} + \mathbf{a}_n), \quad (45)$$

give us the system state in time $t_{n+1} = t_n + \tau$, where τ is a small time interval, if both the state in t_n (i.e. the \mathbf{a}_n , \mathbf{v}_n , \mathbf{w}_n vectors) and the \mathbf{a}_{n+1} acceleration vector are known. If the motion equation is understood as the equilibrium equation in time t_{n+1} , i.e. if

$$\mathbf{R}_{n+1} = \mathbf{M}\mathbf{a}_{n+1} + \mathbf{C}_{NL}(\mathbf{w}_{n+1})\mathbf{v}_{n+1} + \mathbf{K}\mathbf{w}_{n+1} - \mathbf{P}_{n+1} = \mathbf{0}, \quad (46)$$

the solution of equations (44) - (46) will determine the system state in time t_{n+1} . Equation (46) is non-linear and the Newton method is needed to solve it. This equation is treated as non-linear with respect to \mathbf{a}_{n+1} and the associated incremental equation has the form

$$\mathbf{M}_t \delta \mathbf{a} = -\mathbf{R}_{n+1}, \quad (47)$$

where

$$\mathbf{M}_t = \frac{\partial \mathbf{R}_{n+1}}{\partial \mathbf{a}_{n+1}} = .$$

$$\mathbf{M} + \frac{\partial \mathbf{C}_{NL}(\mathbf{w}_{n+1})}{\partial \mathbf{v}_{n+1}} \frac{\partial \mathbf{v}_{n+1}}{\partial \mathbf{a}_{n+1}} + \mathbf{K} \frac{\partial \mathbf{d}_{n+1}}{\partial \mathbf{a}_{n+1}}. \quad (48)$$

Because

$$\begin{aligned} \frac{\partial \mathbf{v}_{n+1}}{\partial \mathbf{a}_{n+1}} &= \frac{1}{2}\tau \mathbf{I}, & \frac{\partial \mathbf{w}_{n+1}}{\partial \mathbf{a}_{n+1}} &= \frac{1}{4}\tau^2 \mathbf{I}, \\ \frac{\partial \mathbf{C}_{NL}(\mathbf{v}_{n+1})}{\partial \mathbf{v}_{n+1}} &= \mathbf{C}_t, \end{aligned} \quad (49)$$

where \mathbf{I} is a diagonal matrix and

$$\mathbf{C}_t = \mathbf{C} - \mathbf{D}_L - 2\mathbf{D}_{NL}(\mathbf{v}_{n+1}, \mathbf{w}_{n+1}), \quad (50)$$

the matrix \mathbf{M}_t is given by

$$\mathbf{M}_t = \mathbf{M} + \frac{1}{2}\tau \mathbf{C}_t + \frac{1}{4}\tau^2 \mathbf{K}. \quad (51)$$

The new approximation of \mathbf{a}_{n+1} denoted by \mathbf{a}_{n+1}^{i+1} is given by

$$\mathbf{a}_{n+1}^{i+1} = \mathbf{a}_{n+1}^i + \delta \mathbf{a}, \quad (52)$$

where the superscript indicates the number of iteration. At the beginning $\mathbf{a}_{n+1}^0 = \mathbf{a}_n$.

The iterations are repeated until the following inequalities are satisfied:

$$\|\mathbf{R}_{n+1}\| \leq \varepsilon_1 \|\mathbf{P}_{n+1}\|, \quad \|\delta \mathbf{a}\| \leq \varepsilon_2 \|\mathbf{a}_{n+1}^{i+1}\|, \quad (53)$$

where ε_1 and ε_2 are the assumed accuracy of calculation.

Starting with some given initial conditions, the system of equations (44) - (46) is solved and the solution of motion equations can be determined by applying the above method recurrently for certain number of intervals τ . The steady state solution can be obtained in this way as well.

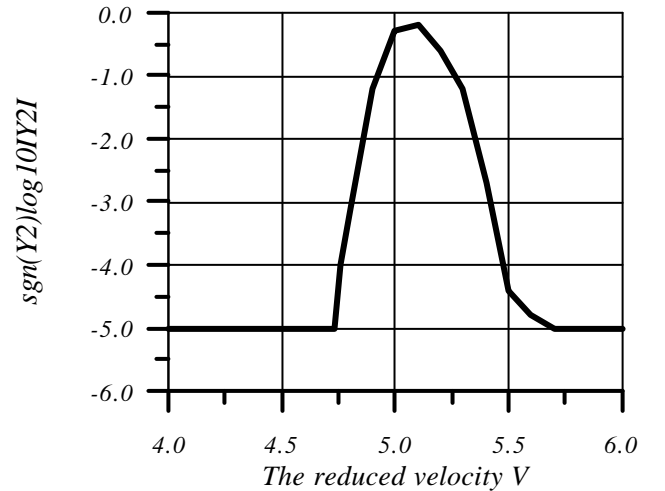


Figure 1: Model parameter Y_2 versus reduced velocity

5. Results of numerical simulations

The fixed-free beam subjected to wind excitation forces is chosen as an example structure. The cylindrical cross-section

of the beam is $D = 1.2 \text{ m}$, the beam length is $L = 32.0 \text{ m}$, and the bending rigidity is $EI = 2.0 \cdot 10^6 \text{ kNm}^2$. Based on the

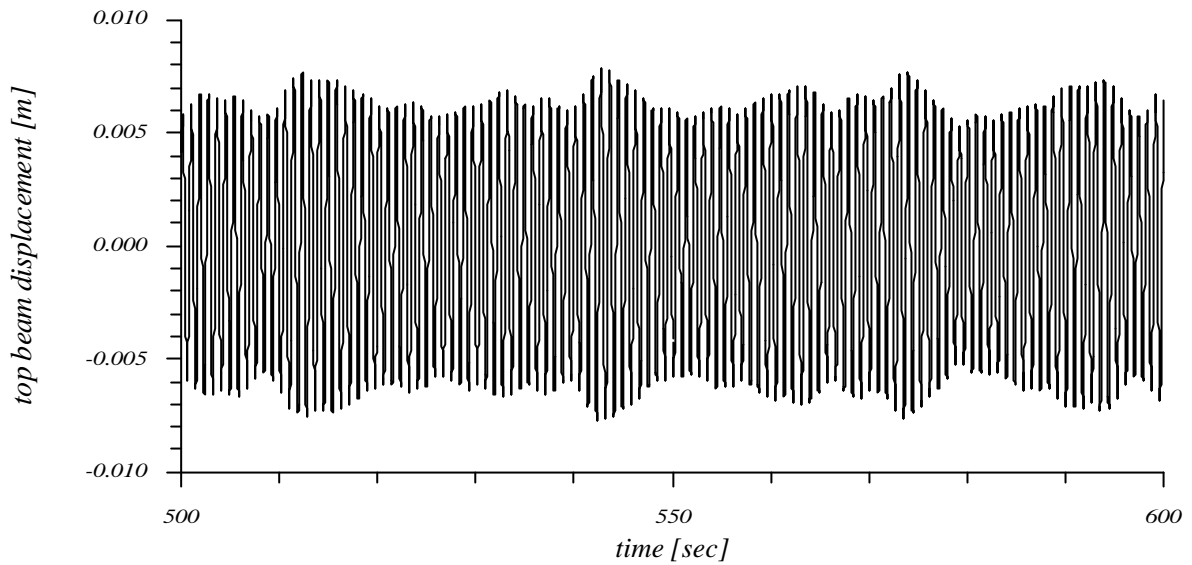


Figure 2. Response of free end of beam ($U=6\text{m/sec}$)

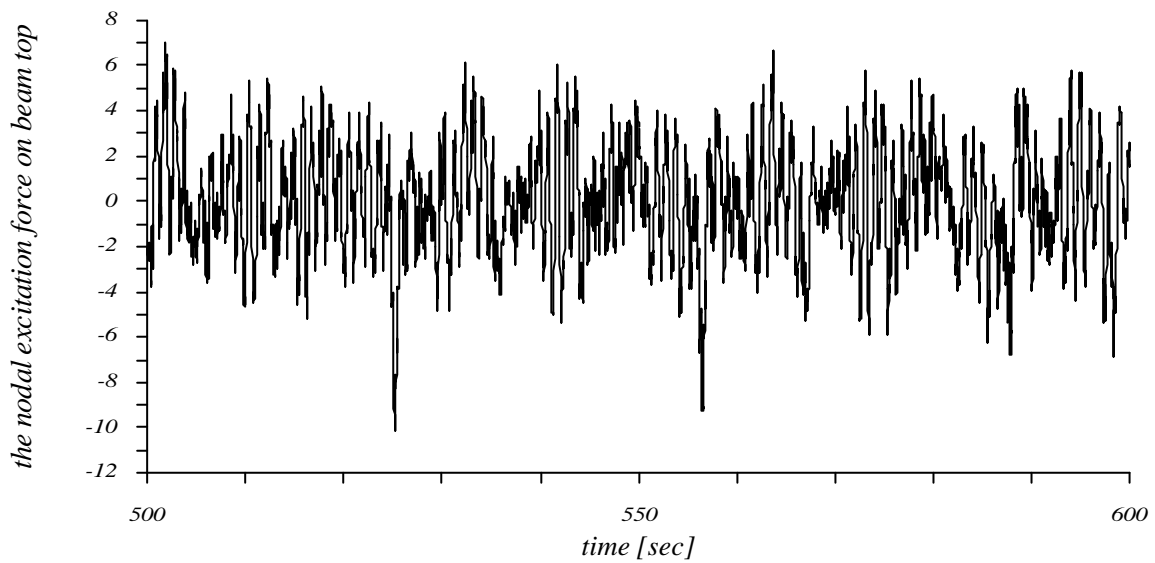


Figure 3. The nodal excitation force versus time ($U=6\text{m/sec}$)

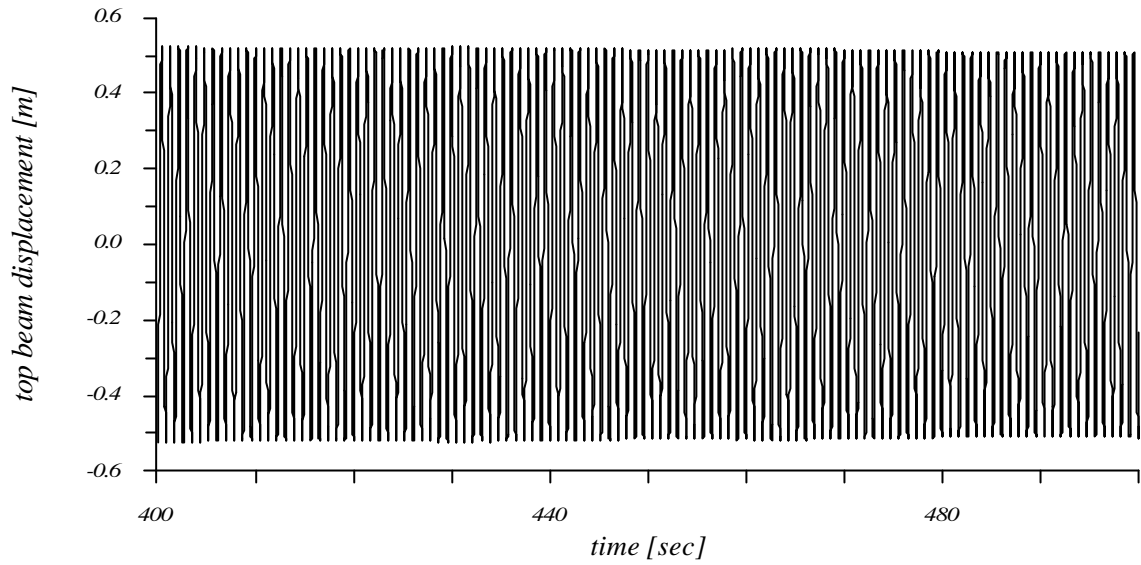


Figure 4. Response of free end of beam ($U=7\text{m/sec}$)

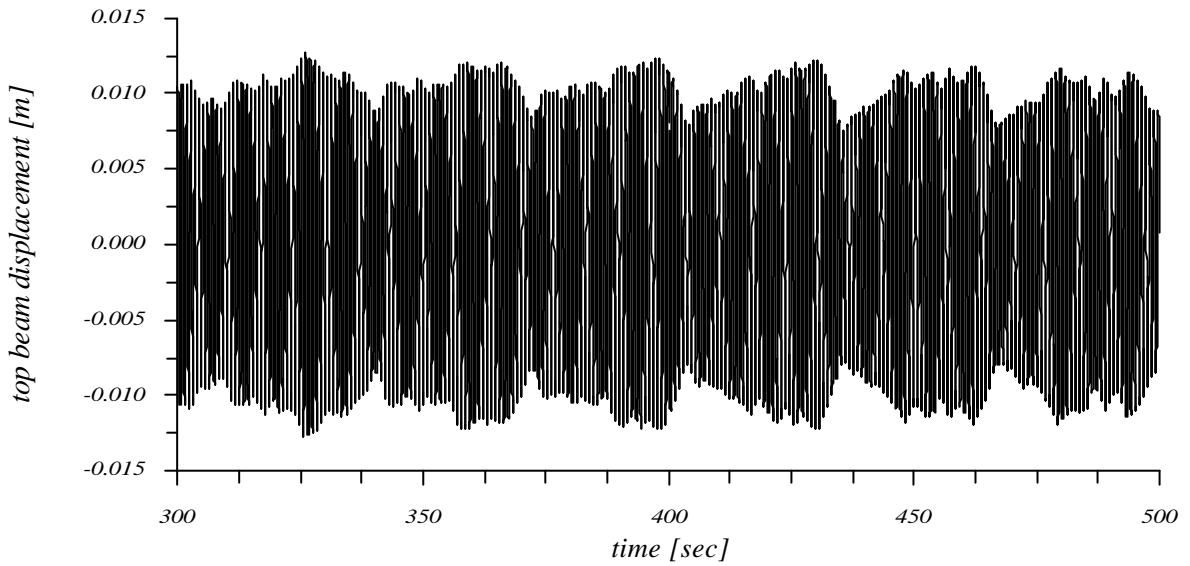


Figure 5. Response of free end of beam ($U=8\text{m/sec}$)

finite element concept, the beam is discretized into ten elements. The first two natural frequencies of the beam are $\omega_1 = 7.2387 \text{ rad/s}$ and $\omega_2 = 45.36 \text{ rad/s}$. Furthermore, the proportional damping properties of the beam are assumed and parameters α and β appearing in equation (4) are chosen in such a way that the non-dimensional modal damping of the first and second modes is equal to 0.003. The air density is $\rho = 1.20 \text{ kg/m}^3$ and the Strouhal number is $S = 0.2$. The mean wind velocity is assumed to be constant along the beam. Moreover, $C_z = 10$, $C_D = 0.4$ and $z_0 = 0.2$. The values of parameters of the lift factor spectral density functions (12) and (13) are $B = 0.1$, $a = 1/3$ and $\bar{C}_L = 0.1$. Three hundred harmonics are taken into account when time histories of $v_i(t)$ are generated and fifty harmonics are used when the $C_{Li}(t)$ histories are generated.

In general, the values of aerodynamic parameters Y_1 and Y_2 are functions of the reduced frequency K or the reduced velocity V . The reduced velocity is defined by $V = U / (f_n D)$ where $f_n = \omega_n / 2\pi$. For a given mean velocity these parameters can be determined, on the basis of experimental results, using methods described in [8], [13] and [14]. For the cylindrical segment, in [15], we can find diagrams on which the model parameters versus the reduced velocity are presented. In the discussed numerical simulations the first parameters i.e. Y_1 is assumed to be nearly constant. $Y_1 = 2$ or $Y_1 = 3$ in all presented cases. The second aerodynamic parameter $Y_2(V)$ versus the reduced velocity is shown in Figure 1, as in paper [15]. However, the model presented in [15] contains also the parametric excitation which is absent in the model presented here. For this reason, Figure 1 gives only the very approximate data for Y_2 .

Below we describe the typical results obtained in the course of extensive numerical simulations. The results refer to the wind with uniform mean velocity, i.e. the mean wind velocity does not change along the beam. In Figure 2 we see the in time vibrations of the free end of beam in the case when the mean wind velocity $U = 6m/s$ (i.e. $V = 4.34$) The value of the parameter Y_2 is chosen to be $Y_2 = -200000.0$. The corresponding nodal excitation force acting on the free end of beam is shown in Figure 3. From Figure 2 we see that the amplitudes of vibrations are small and few harmonics take part in the beam response. As it is described in literature, this is the typical behaviour of beam before the lock-in region.

Now, the behaviour of the proposed model in the lock-in region will be presented. In Figure 4 we see the beam response when the mean wind velocity $U = 7m/s$ (i.e. $V = 5.06$) and when the aerodynamic parameters are $Y_1 = 3$ and $Y_2 = -40.0$. The beam response is periodic and the amplitudes of vibrations are large. The frequency of beam response is approximately equal to the first natural frequency of beam. It is obvious that also in this case the qualitative agreement of the real structure and the proposed numerical model is observed.

Figure 5 presents the results obtained for $U = 8m/s$ ($V = 5.78$). The aerodynamic parameters are $Y_1 = 3$ and $Y_2 = -200000.0$. In this case the mean wind velocity is greater than mean velocities corresponding with the lock-in region. Once again we see the typical behaviour reported in the literature. The beam response contains few harmonics and the amplitudes of vibrations are not too large.

6. Concluding remarks

In this paper the computational model for simulation of vortex-induced vibrations of beams near and in the lock-in region is presented. The main aerodynamic properties of air are taken into account using a model similar to that proposed by Simiu and Scanlan [8]. The extension of this model to beams treated as multi-degree-of-freedom systems is proposed. Several numerical analyses were carried out for beams with cylindrical cross-section. The results of analyses clearly show that the proposed numerical model can produce the typical beam responses which are observed near and in the lock-in region.

Acknowledgements

The paper is partially supported by Grant No. 7 TO7E 027 12 of the Committee of Scientific Research and partially by Grant No. DS-11-001/00 of the Poznan University of Technology.

References

- [1] I. Goswami, R. H. Scanlan and N. P. Jones. Vortex-induced vibration of circular cylinders. Part I: Experimental data. *Journal of Engineering Mechanics*, 119:2270-2287, 1993.
- [2] J.N. Yang and B. Samali. Control of tall buildings in along wind motion. *Journal of Structural Engineering*, 109:50-68, 1983.
- [3] B.J. Vickery and R.I. Basu. Across-wind vibrations of structures of circular cross-section, Part 1, Development of a two dimensional model for two dimensional conditions. *Journal of Wind Engineering and Industrial Aerodynamic*, 12: 49-73, 1983.
- [4] R.I. Basu and B.J. Vickery. Across-wind vibrations of structures of circular cross-section, Part 2, Development of a mathematical model for full scale application. *Journal of Wind Engineering and Industrial Aerodynamic* 12:75-97, 1983
- [5] H. Barhoush, A. H. Namini and R. A. Skop. Vortex shedding analysis by finite elements. *Journal of Sound and Vibration*, 184:111-127, 1995.
- [6] F. A. Dul and J. A. Pietrucha. Numerical analysis of continuous models of structures in nonlinear wind flow using the time-marching approach. In *Proc. of the East European Conference of Wind Engineering, Warsaw, Poland, Part II/1* pages 67-79, 1994.
- [7] R. Lewandowski. Non-linear steady state vibrations of beams excited by vortex-shedding. *Journal of Sound and Vibration*, 2000 (send to publication).
- [8] E. Simiu, R. H. Scanlan. *Wind effects on structures*, 3rd edition, Wiley, New York, 1996.
- [9] R. T. Hartlen and I. G. Currie. Lift oscillator of vortex - induced vibration. *Journal of Engineering Mechanics*, 5: 577-591, 1970
- [10] M. Shinozuka and C.M. Jan. Digital simulation of random processes and its application. *Journal of Sound and Vibration*, 25: 111-128, 1972.
- [11] E. Sarvas, M. Shinozuka and Tsurui. ARMA representation of random processes. *Journal of Engineering Mechanics*, 3, 449-461, 1985.
- [12] H.A. Buchholdt *Structural dynamics for engineers*, Telford, London, 1997
- [13] H. Gupta, P.P. Sarkar and K.C. Mehta. Identification of vortex-induced-response parameters in time domain. *Journal of Engineering Mechanics*, 122:1031-1037, 1996
- [14] F. Ehsan and R.H. Scanlan. Vortex-induced vibrations of flexible bridges. *Journal of Engineering Mechanics*, 116:1392-1411, 1990.
- [15] I. Goswami, R. H. Scanlan and N. P. Jones. Vortex-induced vibration of circular cylinders. Part II: New model. *Journal of Engineering Mechanics* 119: 2288-2302, 1993.